Dynamics, estimation and control of the effects of predator migration between two Lotka-Volterra predator-prey systems

Patricia Apostol, Antonio Arbues, Sandra Wells

***Abstract*— This work proposes a graph-connection model for predatory migration between two Lotka-Volterra predator-prey systems. The resulting proposed system is a generalized Lotka-Volterra model in which the strengths of the two new predatory interactions resulting from the migration are variable and independent. The dynamics of the resulting 4-species system are studied in detail, including its equilibria, local and global stability. State estimation, positive control and optimal control are performed on the system, proving that both system instability and species extinction resulting from the studied predator migration can be effectively tackled and avoided. All numerical simulations, including state estimation and control of the system, are open-source and available at `https://github.com/antonioarbues/lotkavolterra-atic`.**

I. Introduction

A. The Generalized Lotka-Volterra Equations

The generalized Lotka-Volterra model, proposed in [1], is defined by a set of non-linear differential equations that describe the dynamic evolution of n populations of interacting species. These equations are

$$\dot{x} = \mathrm{diag}(x)(Ax + b) := f_{LV}(x) \tag{1}$$

where $x \in \mathbb{R}^n$ represents the population size of the n species, $A = [a_{ij}] \in \mathbb{R}^{n \times n}$ is called the interaction matrix and $b \in \mathbb{R}^n$ is called the intrinsic growth rate. Each individual species i has dynamics

$$\dot{x}_i = x_i \sum_{j=1}^{n} \left(a_{ij} x_j + b_i \right). \tag{2}$$

For a state x to be physically feasible, it must satisfy $x \in \mathbb{R}^n_{\geq 0}$. The interaction terms defined by the coefficients a_{ij} of the A matrix represent the effect on species i from its interaction with species j. If $a_{ij} > 0$, the effect is beneficial on i, if $a_{ij} < 0$ it is damaging on i, and if $a_{ij} = 0$ then j has no effect on the growth of i. In a predator-prey relationship where i depredates j, $aij > 0$, $a_{ji} < 0$. The intrinsic growth rates for each species defined by vector b characterize the behaviour of the population in the absence of any other interacting species. In the case of a prey, an absence of the predator will result in its reproduction and growth over time, and is thus associated with a positive b_i value. For the predator, however, an absence of its prey will lead to it naturally dying and is hence associated with a negative b_i value.

The model additionally assumes that

1) the prey population will find enough food at all times,
2) the food suppy of the predator population depends entirely on the size of the prey population,
3) the rate of change of the population is proportional to its size,
4) the environment does not change in favor of one of the species and
5) predators have endless appetite.

B. Previous Work

Due to the non-linear nature of the Lotka-Volterra model, a wide and ongoing area of research exists in the detailed study of the mathematical and dynamic properties of higher order systems of $n \geq 3$, as explored in, for example, [2], [3], [4]. These include, but are not limited to, the study of fixed and non-fixed point equilibria, their existence, local and global stability, as well as the study of the sometimes appearing chaotic properties. Nevertheless, although certain closed form results and theorems for the aforementioned properties have been developed (see e.g., [5]), analytically characterizing the mathematical properties of these higher order ($n \geq 3$) systems remains complex, is often parameter and dimension limited, and almost always at least partially supported by numerical simulation.

Some recent work exists in which, in addition to studying the detailed and complex mathematical behavior of these systems, biological research has been driven by the interaction of these species in terms of predator-prey migration and/or cross coupling between two or more existing species. The cross-coupling effect between these migrating animals can for instance be easily modelled as a graph where the rate of change in their individual populations can be adjusted by varying the connections and edge weights. [6], for example, investigated the effect of network structure on the dynamic stability of a diffusively coupled Lotka-Volterra system. Nevertheless, the system did not consider any edge weight changes. Instead, migration was only mirrored dynamically by establishing random graph connections with the migrating species.

Various other studies have worked on characterizing the effects of migration on predator prey-systems. A non-graph-based but similar migration model with diffusion was also used by [7] in order to investigate the effect on species coexistence equilibrium as well as on the asymptotic behaviour of the dynamical system. Meanwhile, [8] considered the effects on coexistence of a single predator-prey population when the predators migrate between lands, resulting in no novel graph connections with other species.

When considering the effects of migration, to the authors' knowledge, these and other existing studies have been primarily concerned wih either a single predator-prey system, intraspecific effects or diffusion-based models. Moreover, the focus has been on investigating the intrinsic dynamics and stability of the system, without the implementation of any active state estimation or control methods aiming at stabilizing the system or potentially avoiding species extinction.

With regards to actively controlling a Lotka-Volterra nonlinear system, many methods have been explored. This work is concerned, in particular, with non-negative or positive control, and with optimal control.

Non-negative control is a popular control method that focuses on altering the intrinsic growth rate of one or more species in a system. [9] applied a non-negative control method by developing a Lyapunov-based feedback control law. The control function proposed therein is easy to implement and shows good performance. Nevertheless, the study was limited to a 2-dimensional system. In order to tackle the problem for an n-dimensional system, [10] successfully developed a positive control law based on a classic Lyapunov function while basing the system stability investigation on LaSalle's invariance principle. This latter study forms a basis for the present work.

Optimal control strategies have also been investigated for predator-prey systems. In [11] and [12], the optimal control problem is formulated by adding the hunting effect of the species as the control variable within the considered cost function. These studies showed that when the time horizon is long enough, the optimal strategies are nearly steady state (which is also known as the turnpike property). Here again, however, the study was limited to a 2-dimensional system. As an alternative to this hunter model, [13] proposed a method where an optimal Lyapunov control function is derived for each species by crafting a cost function taking into account perturbed dynamics of the predator-prey system. This method is shown to beautifully stablize the n-dimensional system at its steady state value and will form the basis of further investigation in the current work with regards to tracking of a desired reference in an attempt to combat possible species extinction.

C. *Problem Statement*

This work is concerned with the study of two predator-prey systems where a natural phenomenon allows for the migration of one of the predators to the other predator-prey system. While this can model a wide variety of natural scenarios, it is somewhat inspired by the current challenge faced in Florida, where the burmese python snake is becoming a dangerous superpredator with damaging effects on the local ecosystem by depredating an increasingly large number of species [14]. The two modeled predator-prey systems are the rabbit-snake system and the deer-eagle system. The two predator-prey systems are then connected by the migration of the snake to the deer-eagle system. In the proposed model, species 1 is assigned to the rabbit, species 2 to the snake, species 3 to the deer and species 4 to the eagle.

Two interactions arise from the studied migration: the depredation of deer by snakes, and the depredation of eagles by snakes. These affect four of the system's parameters: a_{23}, indicating the benefit on the snake population from eating deer, a_{24}, indicating the benefit on the snake population from eating eagles, a_{32}, indicating the damage on the deer population from being eaten by snakes, and a_{42}, indicating the damage on the eagle population from being eaten by snakes. For simplicity, it is assumed that $a_{32} = -a_{23}/2$ and $a_{42} = -a_{24}/2$. Then, the connections can be established by setting values of $X, Y \in \mathbb{R}_{\geq 0}$, indicating the strength of the predatory effect of the snake, such that $a_{23} = X$ and $a_{24} = Y$.

The studied system, from now on referred to as "the ecosystem", follows the generalized Lotka-Volterra dynamics in equation (1) with $n = 4$ and the following parameters:

$$A = \begin{pmatrix} 0 & -1/2 & 0 & 0 \\ 1 & 0 & X & Y \\ 0 & -X/2 & 0 & -1/2 \\ 0 & -Y/2 & 1 & 0 \end{pmatrix}, \quad b = \begin{pmatrix} 4 \\ -1 \\ 2 \\ -1 \end{pmatrix}. \quad (3)$$

Parameters for the system (3), as well as the time measure unit, are chosen arbitrarily but keeping the theoretical significance of their ratios and signs. Predators are set to benefit twice as much from their prey than the prey is damaged by the depredation, both predators are set to have the same predatory strength on their prey, both predators die out in the absence of their prey and both preys grow in the absence of their predators, rabbits with a rate twice as high as deer.

The interaction matrix parameters can be represented on a graph as follows:

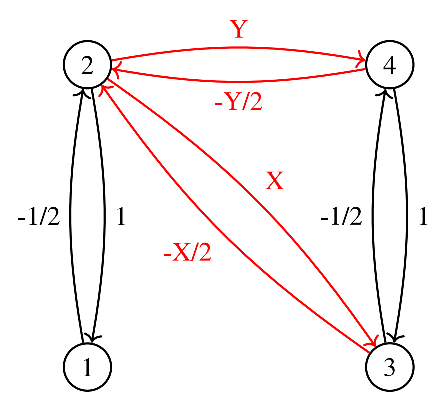

.

The case $X = Y = 0$ corresponds to the state in which the snake does not migrate to the deer-eagle system and both predator-prey systems evolve independently.

The goals of this work are

1) to characterize the dynamics and the equilibria of the ecosystem and derive conclusions on the effects of the graph structure resulting from the interactions in the studied predator migration,
2) to implement a state estimator on the ecosystem and
3) to control the state of the ecosystem using both the real and estimated states.

State estimation is, in fact, a natural implementation for the studied system, as it is unrealistic to assume access to the total number of animals of a given species present in an ecosystem. Moreover, ecosystem control is also motivated in a straightforward manner by the fact that superpredatory effects are unwanted and detrimental on a local ecosystem's biodiversity.

II. Methods

A. Local Stability Methods

Local stability is analyzed here in in terms of local asymptotic stability, which implies that any solution starting close enough to an equilibrium point will remain near to and asymptotically converge to that equilibrium point. In the case of a non-linear system, local asymptotic stability can be assessed by linearizing the system about the equilibrium point. Given a system of the form

$$\dot{x} = f(x) \tag{4}$$

where $f(x)$ is a twice differentiable vector field and x^* an equilibrium in $\mathbb{R}^n$, there exists a linearization M at x^* such that

$$\frac{d}{dt}\Delta x = \frac{\partial f(x)}{\partial x}\Big|_{x^*}\Delta x = M\Delta x \tag{5}$$

where

$$\Delta x = x - x^*. \tag{6}$$

As given in Theorem 15.10 in [15], system (4) is then locally asymptotically stable if all eigenvalues of the matrix M have strictly negative real part. This method is applied to the dynamics $f(x) = f_{LV}(x)$, as given in equation (1).

B. Global Stability Methods

Sufficient conditions for global asymptotic stability of a generalized Lotka-Volterra system are given in Theorem 16.5 in [15] and used throughout the literature (e.g. [16]). The Theorem states that a sufficient condition for global stability on $\mathbb{R}^n_{>0}$ of a generalized Lotka-Volterra system with interaction matrix A, and with a positive unique equilibrium point, is the existence of a diagonal matrix C such that

$$\begin{aligned} CA + A^\top C &\prec 0, \\ C &\succ 0. \end{aligned} \tag{7}$$

This theorem follows from the sufficient conditions for global asymptotic stability given by Lyapunov stability theory (see Theorem 15.4 in [15]) using the Lyapunov function

$$V_{\log-\text{lin},\kappa}(x) = x - \kappa - \kappa\log\left(\frac{x}{\kappa}\right) \tag{8}$$

where $\kappa > 0$, and the complete proof can also be found in [15].

The inequalities in (7) are linear matrix inequalities or LMIs. More specifically, they form a system of LMIs that defines a feasibility problem. This type of problem can be solved with commonly available software such as the LMILAB from MATLAB's Robust Control Toolbox [17], [18]. In particular, LMILAB's `feasp` function computes a feasible solution for the system of LMIs, if it exists, and otherwise indicates that it does not exist. For solving the current problem, let c be the variable vector such that $C = \text{diag}(c)$ and let $L(c)$ be the matrix resulting from stacking $CA + A^\top C$ and $-C$. Then, `feasp` solves the convex program

$$\min\ t \quad \text{s.t. } L(c) \preccurlyeq tI \tag{9}$$

and returns the global minimum of the scalar value t_{min}, as well as, if it exists, a feasible value of c such that all LMI constraints are satisfied. The LMI constraints are then feasible if $t_{min} \leq 0$ and strictly feasible if $t_{min} < 0$.

C. State Estimation Methods

The second contribution of this article is the state estimation method, implemented using an Extended Kalman Filter (EKF) [19] to fuse together the prediction of the known dynamics of the system corrupted by process noise, and the measurements corrupted by measurement noise. To the best knowledge of the authors, there is no previous work that succesfully implements a state estimator for the Lotka-Volterra dynamics.

Here we propose the following formulation, valid for the Generalized Lotka-Volterra dynamics.The considered dynamics (10) and measurements are modeled as corrupted by respectively a process and a measurement noise, assumed to be zero mean multivariate Gaussian noises. Hence, $\boldsymbol{w}_k \sim \boldsymbol{N}(0, \boldsymbol{Q}_k)$, and $\boldsymbol{v}_k \sim \boldsymbol{N}(0, \boldsymbol{R}_k)$. We assume that all the four states are measurable since they all represent the same physical quantity - number of animals in the considered species. Thus, $h(\boldsymbol{x}_k) = \boldsymbol{x}_k$. The dynamics have to be differentiable in order to apply the online linearization required by the EKF. Indeed, this property is fulfilled by the ecosystem equations as in (1). Finally, $\boldsymbol{u}_k$ represents the control vector at the timestep k.

$$\begin{aligned} \boldsymbol{x}_k &= f_{LV}(\boldsymbol{x}_{k-1}, \boldsymbol{u}_k) + \boldsymbol{w}_k \\ \boldsymbol{z}_k &= h(\boldsymbol{x}_k) + \boldsymbol{v}_k = \boldsymbol{x}_k + \boldsymbol{v}_k \end{aligned} \tag{10}$$

The EKF is the nonlinear version of the Kalman filter which linearizes about an estimate of the current mean and covariance. The algorithm has to be run online since it uses a linearization of the dynamics evaluated in the current predicted states and inputs to produce its state estimate as shown in (11).

$$\begin{aligned} \boldsymbol{F}_k &= \frac{\partial f_{LV}}{\partial \boldsymbol{x}}\Big|_{\hat{\boldsymbol{x}}_{k-1|k-1}, \boldsymbol{u}_k} \\ \boldsymbol{H}_k &= \frac{\partial h}{\partial \boldsymbol{x}}\Big|_{\hat{\boldsymbol{x}}_{k|k-1}} \end{aligned} \tag{11}$$

The EKF consists of two steps, recursively applied at every timestep. The first is *Predict* as in (12), and the second is *Update* as in (13).

$$\begin{aligned} \hat{\boldsymbol{x}}_{k|k-1} &= f_{LV}(\hat{\boldsymbol{x}}_{k-1|k-1}, \boldsymbol{u}_k) \\ \boldsymbol{P}_{k|k-1} &= \boldsymbol{F}_k \boldsymbol{P}_{k-1|k-1} \boldsymbol{F}_k^\top + \boldsymbol{Q}_k \end{aligned} \tag{12}$$

$$
\begin{aligned}
&\tilde{\boldsymbol{y}}_k = \boldsymbol{z}_k - h\left(\hat{\boldsymbol{x}}_{k|k-1}\right) \\
&\boldsymbol{S}_k = \boldsymbol{H}_k \boldsymbol{P}_{k|k-1} \boldsymbol{H}_k^\top + \boldsymbol{R}_k \\
&\boldsymbol{K}_k = \boldsymbol{P}_{k|k-1} \boldsymbol{H}_k^\top \boldsymbol{S}_k^{-1} \\
&\hat{\boldsymbol{x}}_{k|k} = \hat{\boldsymbol{x}}_{k|k-1} + \boldsymbol{K}_k \tilde{\boldsymbol{y}}_k \\
&\boldsymbol{P}_{k|k} = \left(\boldsymbol{I} - \boldsymbol{K}_k \boldsymbol{H}_k\right) \boldsymbol{P}_{k|k-1}
\end{aligned} \tag{13}
$$

It is particularly important to keep in mind that including the control input in the estimator dynamics is crucial because of the feedback relationship between controller and estimator, which makes the online estimation and control pipeline successful.

D. Control Methods

1) Positive Control: The first control method that is implemented, the Positive Control, is based on a classical Lyapunov function for Lotka-Volterra systems. As proposed by Grognard et al. [10], the controller is formulated as an additive term in the system dynamics, resulting in (14).

$$\dot{x} = \operatorname{diag}(x)(Ax + b + ku) \tag{14}$$

It is assumed that the control action is always non-negative. The elements of k are not assumed to have the same sign, so that the same control action can benefit one species and harm another one. The considered Lyapunov function is (15), that has time derivative (16), where e is the equilibrium of the system.

$$V(x) = \mathbf{1}^T x - e^T \ln(x) \tag{15}$$

$$
\begin{aligned}
\dot{V} &= \mathbf{1}^T \operatorname{diag}(x)(A(x-e) + ku) - e^T(A(x-e) + ku) \\
&= (x-e)^T ku
\end{aligned} \tag{16}
$$

In order to make $\dot{V} < 0$, and thus ensure global asymptotic stability of the system, the control input u in (17) is defined and used in the controlled dynamics (14).

$$u = \sigma\left(-k^T(x-e)\right) \tag{17}$$

2) Optimal Control: An alternative control method as proposed by El-Gohary et al. [13] is implemented in order to bring the system to a reference value instead of the system's own equilibrium state. This is a capability that the Positive Controller lacks, and which is essential in controlling an ecosystem where a new superpredatory interaction leads the system's equilibrium to the extinction of one or more species. The proposed controller takes the form

$$\dot{x_i} = b_i x_i + \sum_{j=1}^{n} (a_{ij} x_i x_j) + F_i \tag{18}$$

where F_i, $i = 1, 2, ...n$ are the control functions aimed at asymptotically stabilizing the system. The steady states of the controlled model are then determined by the system

$$b_i \bar{x_i} + \sum_{j=1}^{n} (a_{ij} \bar{x_i} \bar{x_j}) + \bar{F_i} = 0. \tag{19}$$

In order to define the system error dynamics, the following variables are introduced:

$$\xi = x_i - \bar{x_i}, V_i = F_i - \bar{F_i} \tag{20}$$

such that

$$\dot{\xi} = b_i \xi_i + \sum_{j=1}^{n} (a_{ij} \bar{x_i} \xi_i + \bar{x_j} \xi_i + \xi_i \xi_j) + V_i. \tag{21}$$

In order to derive an optimal stabilizing control function, we consider minimizing the cost function

$$
\begin{aligned}
J = \frac{1}{2} \int_0^\infty \sum_{i=1}^{n} \Bigg\{ & k_i \xi_i \\
& + \frac{1}{k_i} \left[\sum_{j=1}^{n} a_{ij} \left(\bar{x_i} \xi_i + \bar{x_j} \xi_i + \xi_i \xi_j \right) + V_i \right]^2 \Bigg\} dt,
\end{aligned} \tag{22}
$$

a minimization of the which ($J = 0$) leads to the optimal control function

$$V_i^{opt} = -\left(k_i + \alpha_i\right) \xi_i - \sum_j a_{ij} \left(\bar{x}_i \xi_j + \bar{x}_j \xi_i + \xi_i \xi_j \right). \tag{23}$$

The cost function aims at penalizing the sum of the control effort at each timestep as defined by the control Lyapunov function and the perturbed state. The k_i parameters are considered tuners for the controllers and primarily affect the convergence rate of the system. For further detail and supporting proof of the above optimal Lyapunov function, the reader is referred to the paper by El-Gohary et al. [13].

E. Numerical Simulation Methods

In order to quantitatively observe the behavior of the system, a user-friendly numerical simulator has been built using the programming language `Python3`. The simulator has been developed in an object-oriented fashion, founded on the three core classes representing the Model, the Estimator and the Simulator. The deployable version is directly accessible on GitHub (`https://github.com/antonioarbues/lotkavolterra-atic`) and it is easily usable following the indications in the `Readme`.

The simulator employs the library `NumPy` as its scientific computing support, and makes use of the library `MatPlotLib` in the Plotter class, to handle the generation of the plots. A custom Runge-Kutta 4 algorithm has been used to integrate the dynamics of the system every timestep, an Extended Kalman Filter has been implemented to estimate the states online from noisy dynamics and measurements, and two control algorithms - Positive Controller and Optimal Controller - have been incorporated to close the loop and simulate a realistic control pipeline.

The Positive Controller is implemented for equilibrium tracking, whereas the Optimal Controller for reference tracking. Figure 1 shows the high-level control pipeline in the reference-tracking case.

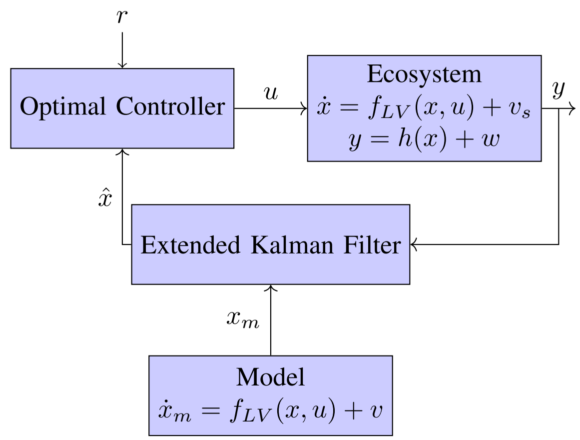

Fig. 1. The reference-following pipeline is implemented as a feedback loop that includes the Estimator and the Controller. Note that the ecosystem is modeled including an additive process noise v_s, that is in general different than the process noise v used in the model. The measurement noise is modeled as the additive term w.

III. Ecosystem Dynamics

A. Ecosystem equilibria

A generalized Lotka-Volterra system defined has a unique positive equilibrium [15],

$$x^* = -A^{-1}b, \tag{24}$$

meaning that all other equilibria of the system have non-positive values for at least one species of the system, which are not feasible in a physical sense. This unique positive equilibrium is thus the one to study for characterizing the behavior of the system.

For $X = Y = 0$, the unique positive equilibrium of the ecosystem is

$$x^* = (1,\ 8,\ 1,\ 4)^\top. \tag{25}$$

This equilibrium is directly altered by the nonzero predation values $X > 0$ and/or $Y > 0$ induced by the snake's migration. The effects of increasing the predatory strengths of the snake X and Y are studied separately, allowing to understand the influence of each of the predatory interactions on the equilibrium state of the four species. The resulting equilibria for increasing values of X and Y are shown in Figures 2 and 3.

Inspection of Figure 2 allows to observe the following for the migration of snakes to the deer-eagle system and subsequent depredation of the deer:

- It results in a decrease of the rabbit equilibrium population. This follows from the snake benefitting from the new ecosystem connection, resulting in being able to exert a stronger predatory effect on its original prey.
- It results in an even more pronounced decrease of the eagle equilibrium population. This follows from the resulting competition relation between snake and eagle. At an X value of 0.5, the equilibrium value of the eagle is its complete extinction.
- The equilibrium values of the snake and deer remain constant. Interestingly, the species involved in the new connection are not affected in this sense, while only their prey and predator, respectively, suffer the consequences.

Inspection of Figure 3 allows to observe the following for the migration of snakes to the deer-eagle system and subsequent depredation of the eagles:

- It results in a decrease of the rabbit equilibrium population. This follows from the snake benefitting from the new ecosystem connection, resulting in being able to exert a stronger predatory effect on its original prey, just as in the previous considered connection. In this case, the rabbit's equilibrium is the first to fall to extinction at a Y value of 0.25. The depredation of eagles by the snake is more damaging to rabbits than the depredation of deer by the snake.
- It results in an increase of the deer population. This follows from the eagle's strength being decreased in the ecosystem, benefitting their prey, the deer.
- The equilibrium values of the snake and eagle remain constant. Interestingly, the species involved in the new connection are not affected in this sense, while only their preys suffer or benefit from the consequences.

Combining an increase in both X and Y combines the effects observed above, proportionally to the increase in each of the parameters. At $X = 0.5$ and $Y = 0.25$, both the eagle's and the rabbit's equilibrium states fall to extinction.

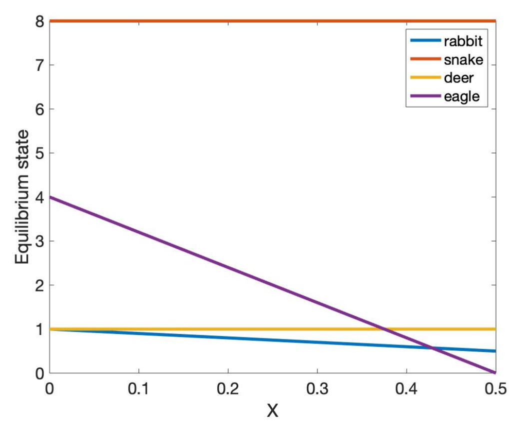

Fig. 2. Variation of the equilibrium state of the ecosystem species when increasing the value X of the snake's depredation of deer.

A next step in the analysis of the ecosystem's dynamics is analyzing the stability of the equilibria obtained in the feasible X and Y range: $X \in [0,\ 0.5)$, $Y \in [0,\ 0.25)$.

B. Stability of the Ecosystem's Equilibria and Induced Behavior

1) Local Stability: The eigenvalues of the linearization matrix M obtained for $X = Y = 0$ are

$$\begin{aligned} \lambda_1 &= 0 + 2i, \quad & \lambda_2 &= 0 - 2i, \\ \lambda_3 &= 0 + \sqrt{2}i, \quad & \lambda_4 &= 0 - \sqrt{2}i. \end{aligned} \tag{26}$$

This case corresponds to two independent predator-prey systems. The conjugate eigenvalues $\lambda_{1,2} = \pm\omega_{1,2} i = \pm 2i$

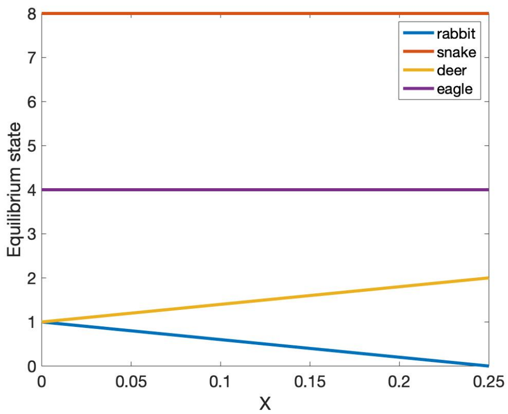

Fig. 3. Variation of the equilibrium state of the ecosystem species when increasing the value Y of the snake's depredation of eagles.

are associated to the equilibrium $x^*_{1,2} = (1,\ 8)$ of the rabbit-snake system, given by the first two states of (27). The conjugate eigenvalues $\lambda_{3,4} = \pm\omega_{3,4}i = \pm\sqrt{2}i$ are associated to the equilibrium $x^*_{3,4} = (1,\ 4)$, of the deer-eagle system, given by the other two states in the same equation. The fact that the eigenvalues are purely imaginary classifies these equilibria as center points. Orbits in these systems, originating in a local neighborhood of the equilibrium point, oscillate around their equilibrium points with oscillation periods of $T_{1,2} = 2\pi/\omega_{1,2} = 2\pi/2 = \pi$ and $T_{3,4} = 2\pi/\omega_{3,4} = 2\pi/\sqrt{2} = \sqrt{2}\pi$, respectively.

The oscillatory behavior found for the disconnected system can be observed as state trajectories in time and as 2-dimensional phase-space projections in Figure 4. In the latter, only the projections on the space $x_1 - x_2$ and $x_3 - x_4$ are closed orbits, as the other variables are not connected through the system and have no established relationship. In this Figure, the oscillation periods for the two systems can be easily observed to match the theoretically found values, as the initial values for the ecosystem's state is very close to the equilibrium point. In Figure 5, initial conditions are set farther away from the equilibrium point and the oscillation behaves less as predicted locally. Nevertheless, both predator-prey systems have a clearly closed orbit in their 2-dimensional phase-space projections.

The linearization matrix M, as well as its eigenvalues, are directly altered by the nonzero predation values $X > 0$ and/or $Y > 0$ induced by the snake's migration. The effects of increasing the predatory strengths of the snake X and Y are studied in order to understand the influence of the predatory interactions on the stability of the equilibrium state of the ecosystem. The resulting eigenvalues of M for increasing values of X and Y are shown in Figure 7. The plots for $\text{Re}(\lambda_2)$ and $\text{Re}(\lambda_4)$ coincide with those for $\text{Re}(\lambda_1)$ and $\text{Re}(\lambda_3)$, respectively, and are thus omitted. Inspection of the data shown in the plots gives that for all values of $X > 0$ and $Y > 0$, $\text{Re}(\lambda_1) = \text{Re}(\lambda_2) > 0$. This implies that the equilibrium of the system is unstable for all feasible

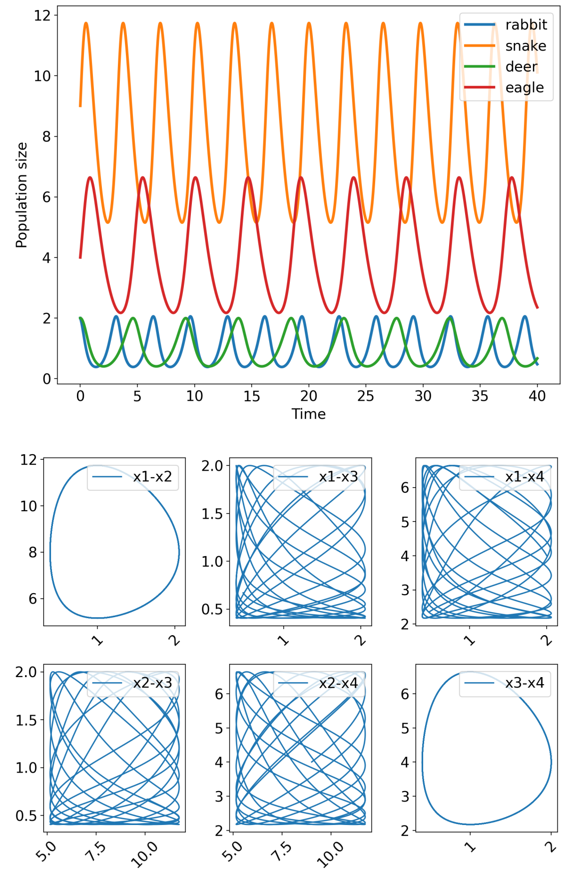

Fig. 4. State trajectories (up) and 2-dimensional phase space projections (down) of the disconnected ecosystem given by $X = Y = 0$, with initial conditions $x(0) = x^* + \mathbf{1}_n$, with x^* given in equation (27), plotted for 40000 iterations.

values of $X > 0$ and $Y > 0$. An example of the trajectories and 2-dimensional phase space projections obtained in this scenario is provided in Figure 6. Clearly, they diverge from the equilibrium point even if started in a close neighborhood of it.

More interestingly, the plots in Figure 7 also show that $\text{Re}(\lambda_i) = 0,\ \forall i$, for $X = 0,\ Y \neq 0$ and $X \neq 0$ and $Y = 0$. The imaginary part of the eigenvalues for $X = 0$ or $Y = 0$, is shown in Figure 8. Clearly, all eigenvalues are purely imaginary eigenvalues, as was the case for the disconnected systems. In these cases, the equilibria are marginally stable, and neither locally asymptotically stable nor unstable.

The analysis of a 4-dimensional system with purely imaginary eigenvalues is barely developed in the literature due to its elevated complexity. Consequently, unlike for 2-dimensional systems, it is not straightforward to state that resulting orbits around the equilibrium point are closed. Nevertheless, simulating the ecosystem's dynamics in phase space shows a similar behavior to that of 2-dimensional center points. In a local neighborhood of the equilibrium point, orbits remain in a bounded region and could be hypothesized to be closed periodic orbits or even chaotic aperiodic orbits. This simulation, for the example values $X = 0$ and $Y = 0.2$,

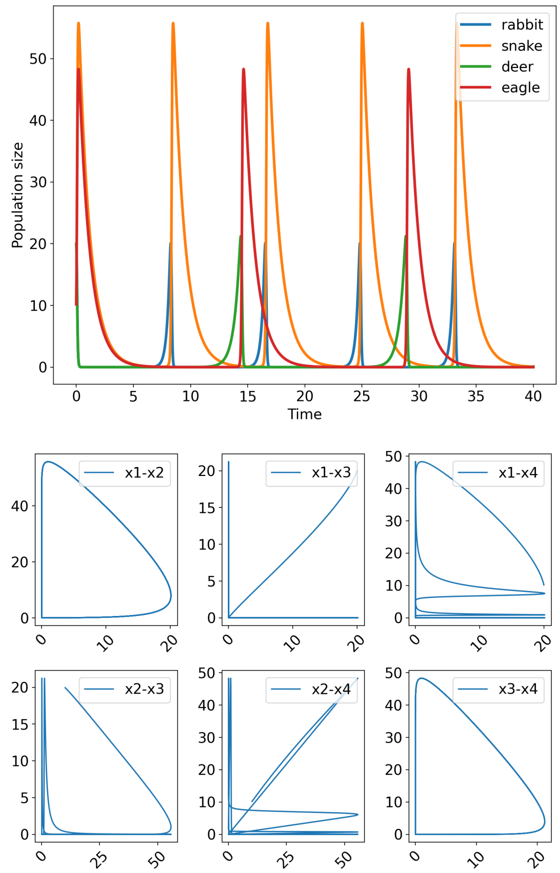

Fig. 5. State trajectories (up) and 2-dimensional phase space projections (down) of the disconnected ecosystem given by $X = Y = 0$, with initial conditions $x(0) = (20,\ 10,\ 20,\ 10)^\top$, plotted for 40000 iterations.

is shown in Figure 9 for initial conditions at varying distances from the ecosystem's equilibrium point. The smaller the value of d, the more notorious it is that the orbits are bounded, potentially closed and, quite honestly, beautiful!

An example of a time trajectory corresponding to the phase-space plots in Figure 9 is provided in Figure 10. The rest are similar and omitted for space.

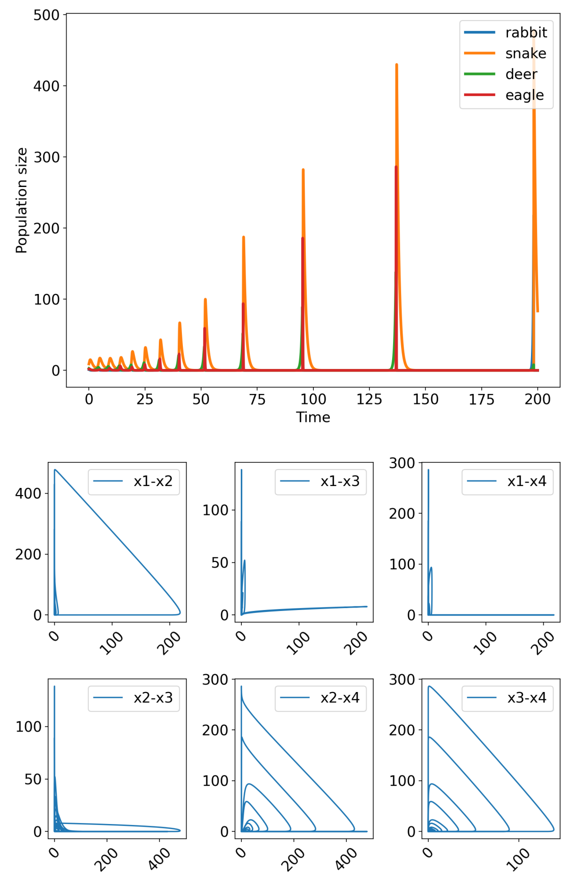

Fig. 6. State trajectories (up) and 2-dimensional phase space projections (down) of the ecosystem with $X = 0.4$ and $Y = 0.2$, with corresponding equilibrium state $x^* = (0.12,\ 8,\ 1.8,\ 0.8)^\top$, and initial conditions $x(0) = x^* + \mathbf{1}_n$, plotted for 200000 iterations.

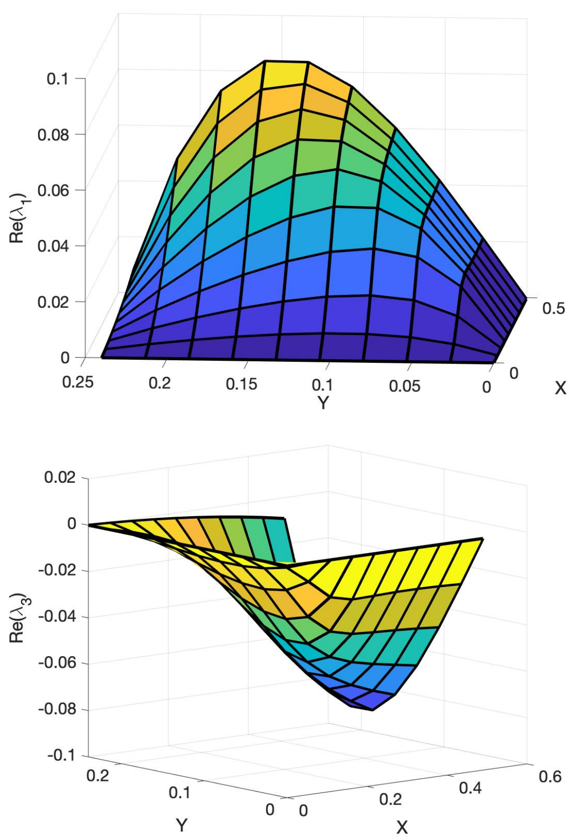

Fig. 7. Variation of Re(λ_1) (up) and Re(λ_3) (down) with changing values of X and Y.

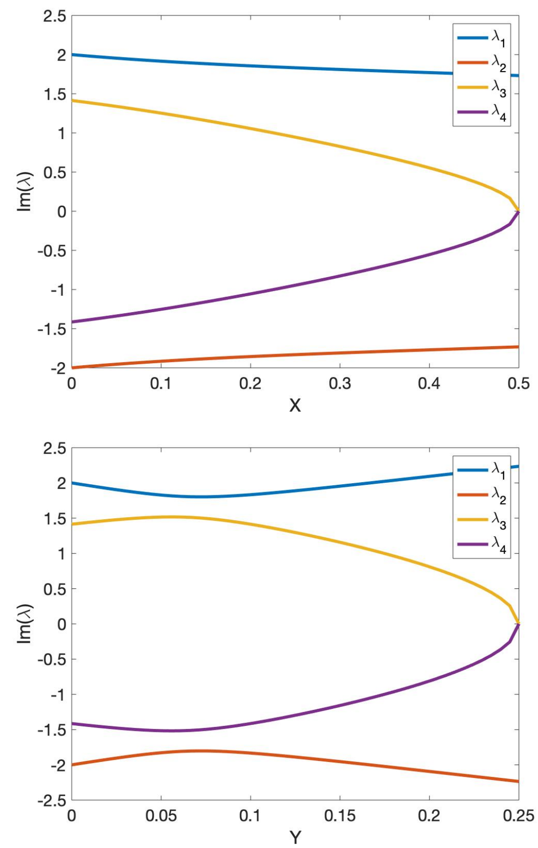

Fig. 8. Variation of the value of Im(λ_i), $\forall i$, with changing values of X (up) and Y (down), and fixed values $Y = 0$ and $X = 0$, respectively.

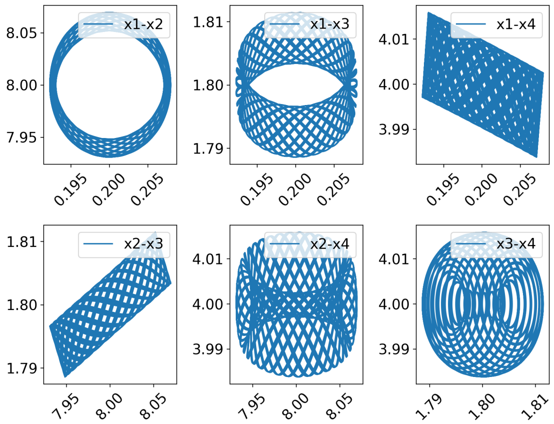

(a) $d = 0.05$

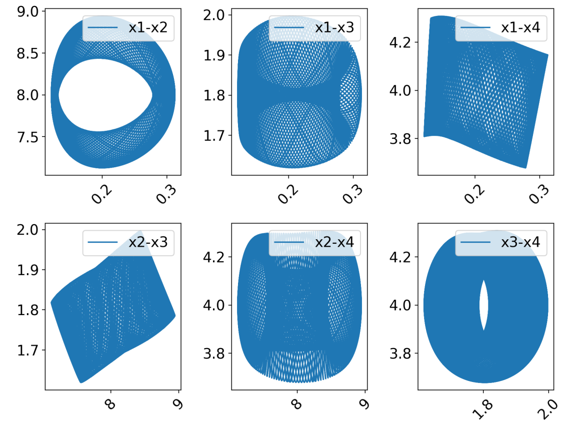

(b) $d = 0.1$

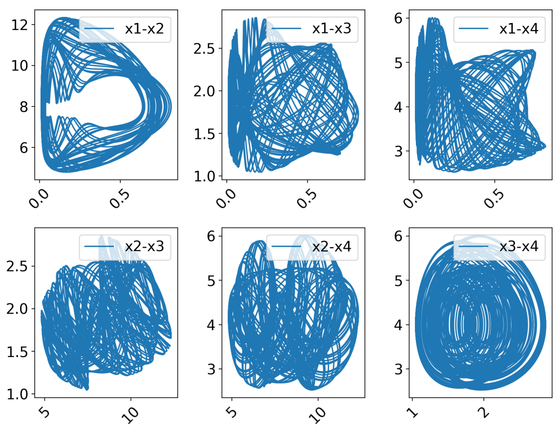

(c) $d = 0.5$

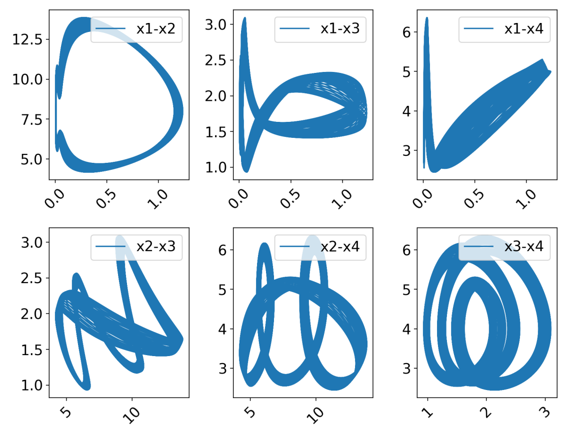

(d) $d = 1$

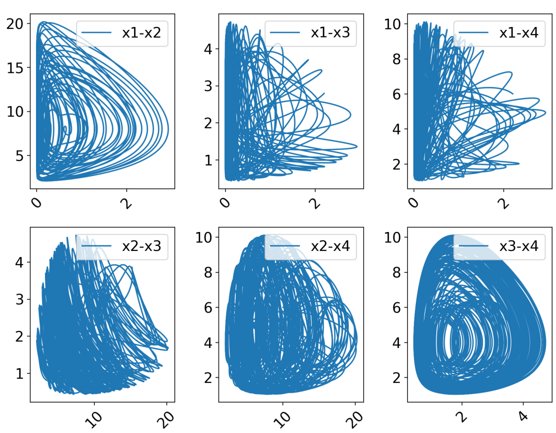

(e) $d = 2$

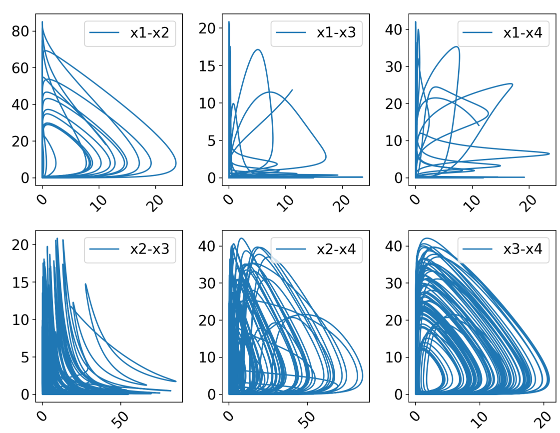

(f) $d = 10$

Fig. 9. 2-dimensional projection phase space plots for the ecosystem with $X = 0$ and $Y = 0.2$, with corresponding equilibrium state $x^* = (0.2,\ 8,\ 1.8,\ 4)^\top$, and initial conditions $x(0) = x^* + d\mathbf{1}_n$, at varying distances d from x^*, plotted for 400000 iterations.

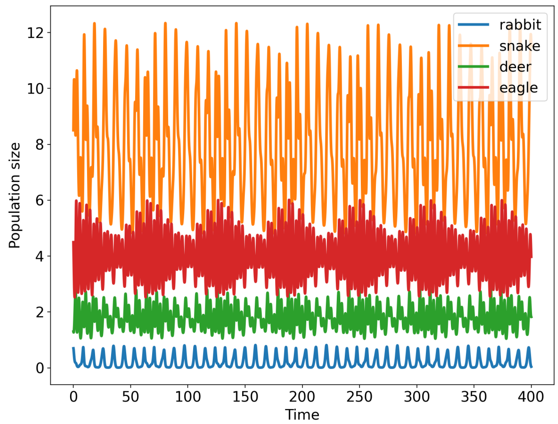

Fig. 10. State trajectories corresponding to the phase space plot in Figure 9 for the case $d = 0.5$.

2) Global Stability: The obtained results for the studied system are that there exists no combination of feasible values of X and Y such that the sufficient condition in equation (7) is satisfied. This means that global asymptotic stability cannot be ensured for the system. In particular, `feasp` returns $t_{min} \approx 0$ in all studied cases. Given that it has been found in the previous section that there are no feasible, nonzero values of X and Y such that the system is locally stable, this result is expected, as local stability is a necessary condition for global stability.

Global asymptotic stability is a powerful property of a dynamical system. For the studied system, it would imply a guarantee that no species grows uncontrollably, that no species becomes extinct and that all states asymptotically converge to the system's equilibrium state values. The absence of this behavior in the studied system justifies the implementation of a controller such that global asymptotic stability of the system is ensured.

IV. Ecosystem State Estimation

The performance of the Extended Kalman Filter as state estimator has been implemented together with the previously described control methods in Section II-D and further discussed in Section V. The estimator proves to be very well suited to the Generalized Lotka-Volterra dynamics in terms of convergence. This is well visible both in Figure 12 and Figure **??**. The fact that the model used for the estimation and the dynamics of the system solely differ by a noise term is for sure helpful for the convergence of the filter - for which the convergence is not guaranteed if the process is not well modeled. Moreover, the EKF shows a very good performance in terms of state estimation in comparison to the states of the noisy Ground Truth.

Figure 13 shows that the EKF results to be quite dependent on the tuning of the two covariance matrices $\boldsymbol{Q}$ and $\boldsymbol{R}$. In fact, the estimated states keep diverging over time compared to the Ground Truth. However, this can be easily solved iterating the tuning process, changing the two previously mentioned matrices.

V. Ecosystem Control

Initially, a Positive Controller is implemented to stabilize the system about its equilibrium point. Subsequently, with the aim of outperforming the Positive Controller, an alternative Optimal controller is added. The Positive Control aims at quick tracking and convergence to the system's natural equilibrium state. Meanwhile, it is shown that the Optimal Controller may also be used also used as a reference tracker, and can thus in theory tackle a potential non-positive equilibrium and thereby species extinction.

A. Positive Control

The equilibrium of the system for the considered values of $X = 0.4$ and $Y = 0.2$ is

$$x^* = (0.12,\ 8.0,\ 1.8,\ 0.8)^\top . \tag{27}$$

Figure 6 shows how, even close to the equilibrium, the system's dynamics are divergent, justifying the choice of ecosystem parameters for which we simulate the controller.

1) Without sate estimation: As displayed in Figure 11, the tuned controller achieves a great equilibrium stabilization performance with a very low overshoot in only some of the states, and a very low convergence time.

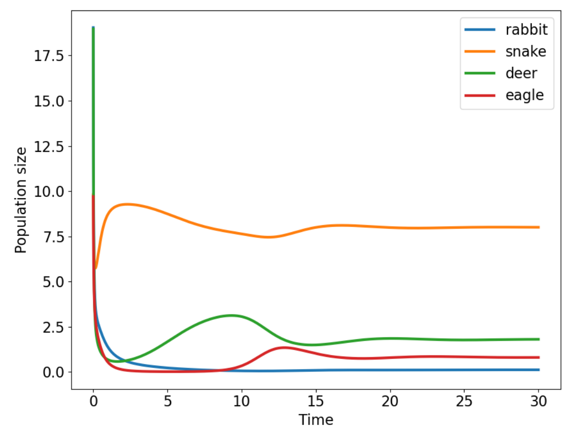

Fig. 11. Positive Controller applied to the noise-free Ground-Truth in order to isolate solely its behavior. The controller converges to the equilibrium $x^* = (0.12,\ 8.0,\ 1.8,\ 0.8)^\top$ and uses the parameters $X = 0.4, Y = 0.2$, $x(0) = (20,\ 10,\ 20,\ 10)^\top$, $k_i = 1.0, \forall i$, plotted for 30000 iterations.

2) With state estimation: The plots for the Positive Controller with the state estimation can be seen in Figure 12 and 13, the details of which have already been discussed in Section IV. Clearly, in both cases where noise is added into the simulator and Kalman filter, the controller still manages to successfully track the reference value for the tuned estimated variance of the EKF.

B. Optimal Control

The Optimal Controller performance has been assessed in two cases. The first considers the original system with a positive equilibrium as defined in (27). For the second, in order to assess the controller's performance in the case of

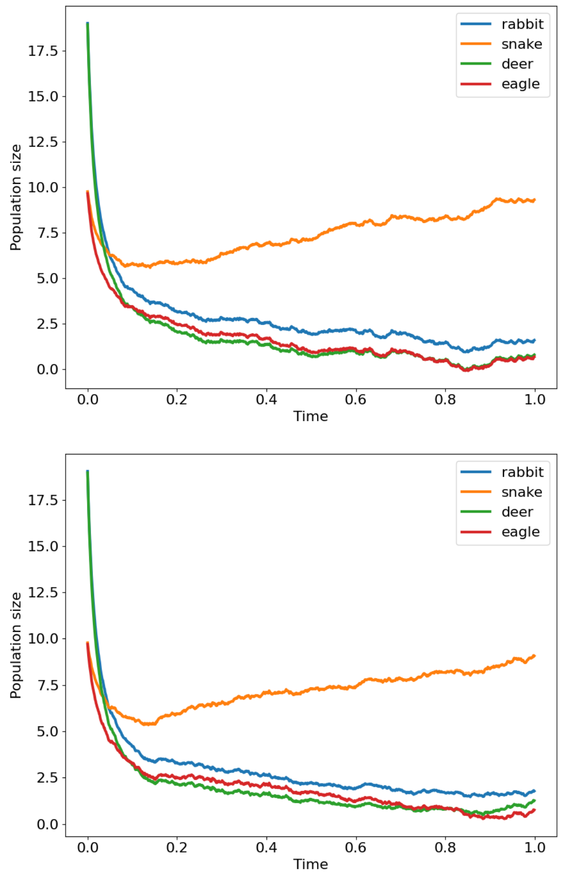

Fig. 12. State trajectories of the Ground Truth with Positive Controller (up), and state trajectories of the complete pipeline with the Estimator in the loop (down). The controller drives the system to the equilibrium and the estimated states are comparable to the Ground Truth. The used parameters are $X = 0.4$, $Y = 0.2$, $x(0) = (20,\ 10,\ 20,\ 10)^\top$, and all the diagonal terms of Q and R are set < 0.03, close to the simulator noise convariance values.

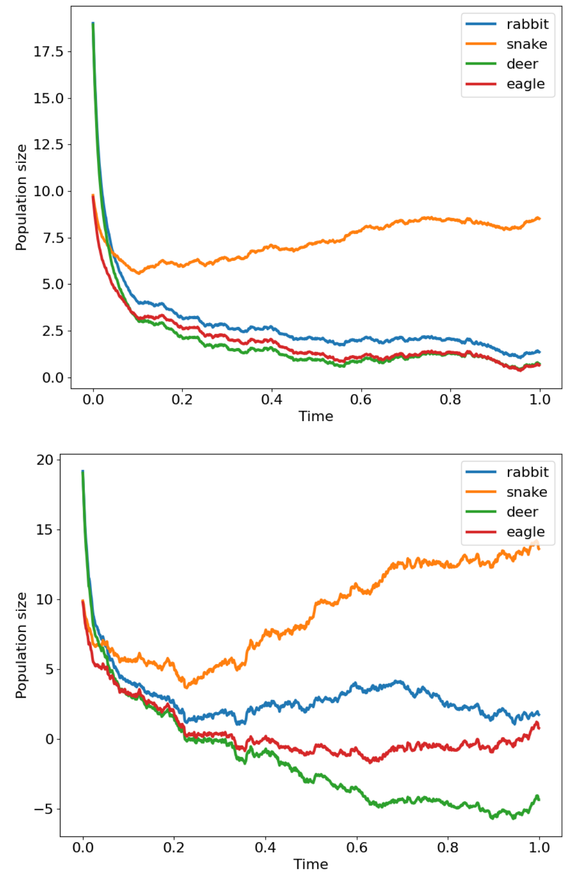

Fig. 13. State trajectories of the Ground Truth with Positive Controller (up), and state trajectories of the complete pipeline with the Estimator in the loop (down). The estimated variance of the EKF model is not tuned. Hence, the estimator results quite inaccurate. The used parameters are $X = 0.4$, $Y = 0.2$, $x(0) = ((20,\ 10,\ 20,\ 10)^\top$, and $Q_{11} = 0.2$, $R_{11} = 0.1$, whereas all the other diagonal terms of Q and R are set < 0.03.

species extinction, the following partially negative equilibrium is considered for $X = 0.7, Y = 0.2$:

$$x^* = (0.06,\ 8.0,\ 1.8,\ -1.60)^\top. \tag{28}$$

For both the positive and negative equlibirum as well as in the simulation with and without the state estimator, the Optimal Controller aims at tracking the reference value

$$r = (2.0,\ 3.0,\ 4.0,\ 1.0)^\top \tag{29}$$

in which extinction of any species is avoided.

1) Without state estimation: The plot showing the controller tracking performance for both a positive and negative equilibrium parameters can be seen in Figure 14 and Figure 15, respectively. In both cases, the controller achieves perfect tracking of the desired reference point. Hence, the Optimal Controller proves here to be successful in preventing the eagle's extinction, which was mathematically mirrored here by the negative equilibrium value of -1.60.

2) With state estimation: The plots of the Optimal Controller state trajetories of the Ground Truth and complete pipeline with the estimator can be seen in Figure **??** and

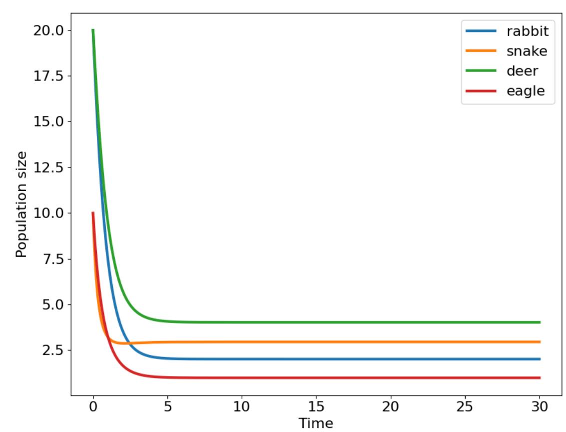

Fig. 14. Time evolution of connected ecosystem with the Optimal Controller: $X = 0.4, Y = 0.2$, $x^* = (0.12,\ 8.0,\ 1.8,\ 0.8)^\top$, and initial conditions $x(0) = (20,\ 10,\ 20,\ 10)^\top$, plotted for 50000 iterations with $k_1 = 1.3$, $k_2 = 1.2$, $k_3 = 1.2$, $k_4 = 1.1$

16 respectively. As for the Positive Controller, in both cases where noise is added into both the simulator and Kalman

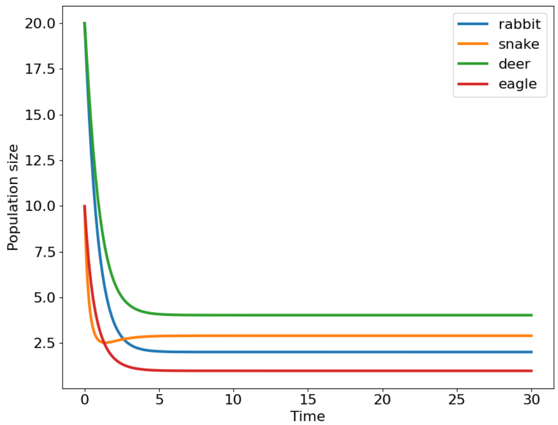

Fig. 15. Time evolution of connected ecosystem with the Optimal Controller at a negative equilibrium: $X = 0.7, Y = 0.2$, $x^* = (0.06,\ 8.0,\ 1.8,\ -1.6)^\top$, and initial conditions $x(0) = (20,\ 10,\ 20,\ 10)^\top$, plotted for 50000 iterations with $k_1 = 1.3$, $k_2 = 1.2$, $k_3 = 1.2$, $k_4 = 1.1$.

filter, the controller still manages to successfully track the reference value for the tuned estimated variance of the EKF.

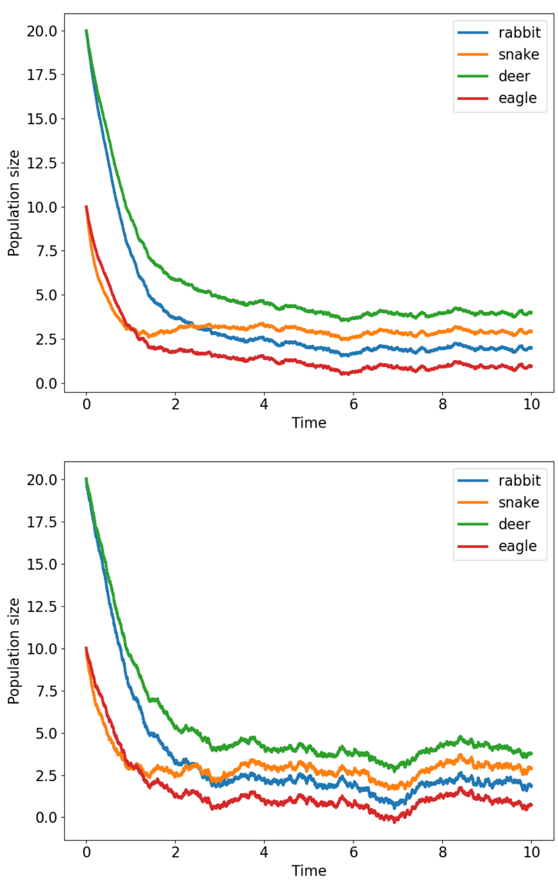

Fig. 16. State trajectories of the Ground Truth with Optimal Controller (up), and state trajectories of the fully integrated estimator pipeline (down). The used parameters are $X = 0.4, Y = 0.2$, $x^* = (0.12,\ 8.0,\ 1.8,\ 0.8)$, and initial conditions $x(0) = (20,\ 10,\ 20,\ 10)^\top$, plotted for 10000 iterations with $k_1 = 1.3$, $k_2 = 1.2$, $k_3 = 1.2$, $k_4 = 1.1$, and reference from equation (29).

C. *Comparison between the two controllers*

In its implementation, the Positive Controller focuses on altering the intrinsic growth rate of the species uniformly. There is a single control input for all the states. When $u > 0$, it can be interpreted as increasing the species' reproduction rate by, for instance, assisting in the their reproduction. When $u < 0$, it can be intepreted to take the physical form of, for instance, a pesticide, a hunting action or an unfavorable light/temperature exposure.

In contrast, the Optimal Controller is purely additive. The control action F_i is different for each species and it represents, for $F_i > 0$, a direct reintroduction of the given number of specimens of the species i into the system, and for $F_i < 0$ a direct elimination of the given number of specimens of the species i. These control actions take values at every timestep by directly considering the error dynamics from the desired steady state value.

Given how the Positive Controller affects the intrinsic growth rate of a species through an external parameter as previously described, in practice, this controller might be more complicated to implement than the Optimal Controller, which directly controls the number of species reintroduced or killed per timestep. Moreover, the Optimal Controller has displayed excellent tracking behaviour and may thus be ideally used for stabilizing the ecosystem at a steady state other than the equilibrium point thereby potentially tackling species extinction driven by a strong superpredatory interaction.

VI. Conclusions

A first contribution of this work has been analyzing the dynamics, local and global stability of two Lotka-Volterra predator-prey systems connected by one or two new predatory interactions. This allows to gain insight on the effects of migratory and/or superpredatory species that interact with new predator-prey systems. It is found that species coexistence is possible in this scenario for a given range of predatory strengths X and Y. Subsequently, after certain values of the predatory strengths, the prey of the migrating predator, and the predator of the non-migrating system, are the first to become extinct. It is also found that both the disconnected systems and the connected system where only one new feasible depredation is established are locally marginally stable systems with bounded orbits around their positive equilibrium. Conversely, connecting the systems with both of the new feasible predatory interactions always results in an unstable behavior with trajectories diverging from the system's positive equilibrium. For none of the aforementioned scenarios is the system found to be globally asymptotically stable.

A second contribution of this work has been the state estimation of a Lotka-Volterra system. To the authors' knowledge, this is the first time it has been performed. The proposed approach has been an Extended Kalman Filter. This estimator has additionally been implemented in a Python framework, showing very satisfactory results on our system.

A third contribution of this work has been the control of the connected predator-prey system, both from a positive control and an optimal control perspective. While both these approaches have been proposed and implemented before in the literature, they (nor any other control method) had not been implemented on a system where new migratory and/or superpredatory interactions are considered. Moreover, the optimal control method implemented had only been used previously for steady state stabilization, while we have shown it is also successful in reference tracking. The significance of this reference tracking result lies in that it has the potential of avoiding the extinction of a species, when it is induced by the new studied predatory interactions. Both control methods have been implemented with and without the implemented state estimator.

Finally, a complete and easy-to-use simulator, including the estimation and control pipeline, are provided as open-source software available for use in further research.

Natural continuations of this work might include considering a different set of system parameters adapting to a different natural scenario, increasing the complexity of the ecosystem and implementing controllers that act at a lower frequency, thus potentially improving their real-world applicability.

REFERENCES

[1] V. Volterra. Variations and Fluctuations of the Number of Individuals in Animal Species living together. ICES Journal of Marine Science, 3(1), 3-51, 1928.

[2] V. Kozlov and S. Vakulenko. On Chaos in Lotka-Volterra systems: an analytical approach. London Mathematical Society, 26(8), 2013.

[3] M. H. Mohd, N. A. Azman, and N. A. Aziz. Alternative Stable States and Limit Cycles in a Three-Species Ecological System, AIP Conference Proceedings 2266, 2020.

[4] X. Li, C. Tang and X. Ji. The Criteria for Globally Stable Equilibrium in n-Dimensional Lotka- Volterra Systems, Journal of Mathematical Analysis and Applications 240, 600-606, 1999.

[5] J. Hofbauer, K. Sigmund. Evolutionary Games and Population Dynamics. Cambridge: Cambridge University Press, 1998.

[6] T. Nagatani. Diffusively coupled Lotka-Volterra system stabilized by heterogeneous graphs, Physica A., 2019.

[7] Q. Yang. Qualitative analysis of a Lotka- Volterra predator-prey system with migration. Journal of Mathematical Analysis and Applications, 472(1), 2019.

[8] T. Nagatani, K. Tainaka and G. Ichinose. Effect of directional migration of Lotka-Volterra system with desert, Biosystems, 162, 75-80, 2017.

[9] M. Meza, A. Bhaya, E. Kaszkurewicz. Controller design techniques for the Lotka-Volterra nonlinear system, Sba Controle Automação 16 (2), 2014.

[10] F. Grognard, J.-L. Gouzè. Positive control of Lotka-Volterra systems.IFAC Proceedings Volumes, 38(1), 2005.

[11] A. Ibañez. Optimal Control of the Lotka-Volterra system: turnpike property and numerical simulations, Journal of Biological Dynamics, 11(1), 25-41, 2016.

[12] A. Ibañez. Optimal control and turnpike properties of the Lotka-Volterra model. Master thesis, 2016.

[13] A. El-Gohary, M.T. Yassen. Optimal control and synchronisation of Lotka-Volterra model, Chaos, Solitons and Fractals, 12(11), 2087-2093, 2000.

[14] G. Steffens. The snakes that ate Florida, Smithsonian Magazine, August 2019. https://www.smithsonianmag.com/science-nature/snakes-ate-florida-180972534/

[15] F. Bullo. Lectures on Network Systems. Kindle Direct Publishing, 1.4 edition, 2020. With contributionsby J. Cortes, F. Dorfler, and S. Martinez.

[16] A. Hastings. Global stability in Lotka-Volterra systems with diffusion. J. Math. Biology 6, 163–168, 1978.

[17] G. Balas, R. Cihang, A. Packard, and M. Safonov. Robust Control ToolboxTM 3 user's guide. January 2012.

[18] P. Gahinet, A. Nemirovski, A.J. Laub, and M. Chilali. LMI Control Toolbox user's guide. The MathWorks, Inc., May 1995.

[19] A. H. Jazwinski. Stochastic Processes and Filtering Theory. Academic Press, New York, NY. 1970.